19th Brazilian Congress of Thermal Sciences and Engineering
November 6th–10th, 2022, Bento Gonçalves - RS - Brazil

ENC-2022-0230
NUMERICAL STUDY OF ARTILLERY AMMUNITION RANGE INCREASE USING BASE BLEED TECHNOLOGY

Thallyo Yuri Caetano Pereira
Wallace Ramos Rosendo da Silva
André Luiz Tenório Rezende
Rubenildo Pithon Barros
Instituto Militar de Engenharia, Rio de Janeiro, RJ, Brazil
thallyo.pereira@ime.eb.br, wrosendoeng@gmail.com, arezende@ime.eb.br, rpbarros@ime.eb.br

Abstract. *Artillery is the main combat support for maneuver forces and, with the evolution of the art of war and defense strategies, extending the range of these heavy weapons ammunition has become increasingly important. As increasing the pressure at the base of the projectile is the most efficient method of extending munition range, the base bleed technology, a system that can be incorporated downstream of a munition and increases its range by injecting gases at the rear by decreasing recirculation zones behind the projectile and reducing base drag, becomes an optimal solution. However, while this technology is already widely produced and used by several countries, there is still a need for knowledge production in Brazil to develop bleed-based systems for the different calibers of artillery endowment. Ergo, this paper analyzes the increase in ammunition range through the use of a base bleed system. The study is carried out from the ballistic trajectory obtained through the modified point-mass trajectory model, proposed by NATO Standard STANAG 4355, and from the application of the fourth-order Runge-Kutta numerical method. First, numerical simulations were performed for the projectile without base bleed with the objective of validating the code. Afterwards, results were obtained to study the influence of the base bleed system parameters for the range increase. The computer codes developed allowed the modeling of the trajectory for firing angles of up to 75 degrees, within the context of artillery. The final results showed promising results to range increase, but further studies are needed to properly simulate real scenarios.*

Keywords: *artillery ammunition, base bleed, trajectory simulations*

1. INTRODUCTION

Artillery is the main combat support for maneuver forces and, with the evolution of the art of war and defense strategies, the increase in the range of these heavy weapons ammunition has become increasingly important. However, as designing, producing and distributing new weapons are costly and time-consuming processes, extended range munitions become very interesting alternatives.

The development of munition generally has range increase and accuracy improvement as requirements. For this reason, while most of the drag over the projectile results from the friction between the air and the warhead at supersonic speeds, increasing the range by altering the ammunition geometry is complex, as shifting the center of mass can reduce its accuracy (Anderson *et al.*, 1976).

The base drag, which comes from the pressure difference in the rear region of the projectile, can be reduced by increasing the pressure at the base of the ammunition. So, the base bleed (BB) technology was developed in Sweden, a system that can be incorporated into the base of the ammunition with the aim of reducing the base drag by increasing the temperature in the posterior region and, consequently, increasing the range (Anderson *et al.*, 1976).

1.1 Motivation and Objectives

Even though the base bleed technology is already widely produced and used in several countries, the few bleed-based ammo available in Brazil comes from importation. And, according to Rosendo (2020), despite efforts to produce a national BB system for the 114,3 mm munition, Brazilian defense industry still doesn't master the technology to develop and produce the system for the different calibers of artillery endowment. Thus, given the value of extended range munitions to the recovering of artillery materials, there is still a need for knowledge production about this technology in order to develop national base bleed munitions.

Therefore, this paper analyzes the increase in ammunition range through the use of a bleed-based system. The study is carried out from the ballistic trajectory obtained through the modified point-mass trajectory model, proposed by NATO Standard STANAG 4355, and from the application of the fourth-order Runge-Kutta numerical method. The objective is to analyze the influence of the base bleed system over the trajectory, with the aim of increasing the ammunition range.

2. LITERATURE REVIEW

In this section, in order to better understand the base bleed technology and guide the next activities of this study, important concepts to the extension of ammunition range are presented.

As described previously in section 1, due to the evolution of modern combat, increasing the range of artillery has become a necessity. However, considering the resources needed to produce and distribute new weapons, extended range ammunition is the best way to achieve this objective. Among the various ways to extend the range of an ammunition, the ones that stand out are the Rocket-Assisted Projectiles (RAP) and the reduction of drag (Anderson *et al.*, 1976).

The RAP works based on the actuation of a rocket engine, that produces a thrust large enough to increase the speed of the projectile after launch. Despite promoting a greater range increase, the independent propulsion system takes up more space and, as a result, accommodates less explosive charge. In addition, another disadvantage is the lower precision, since the thrust generated and the mass variation cause changes in the center of pressure during flight (Anderson *et al.*, 1976).

For this reason, drag reduction is usually the most efficient method to increase range and, as shown in Fig. 1, can be achieved by various means. It is important to note that the drag can be categorized as wave drag, due to friction between fluid and surface, and as base drag, caused by the pressure difference at the base of the projectile (Anderson *et al.*, 1976).

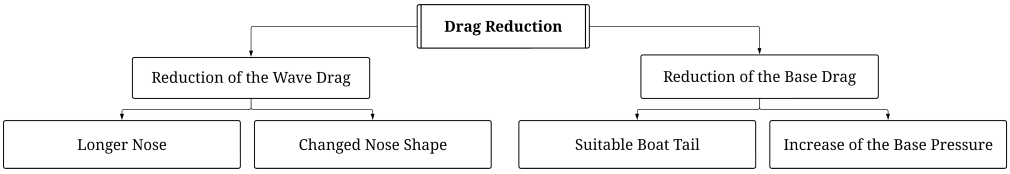

Figure 1. Drag reduction methods according to Anderson *et al.* (1976)

2.1 Drag Reduction

The wave drag is directly associated with the projectile geometry, which can be optimized through Computational Fluid Dynamics (CFD). However, in addition to being limited by the weapon for which the ammunition is designed, changing the geometry in such a way as to effectively reduce the total drag shifts the projectile's center of mass and negatively impacts its accuracy (Dali and Jaramaz, 2018).

Geometry also influences the base drag, since the pressure difference at the base is closely related to the shape of the projectile's posterior region. However, as increasing the length or angle of the boat tail can increase frictional drag, it is not simple to achieve the suitable boat tail described in Fig. 1 (Dali and Jaramaz, 2018).

Therefore, increasing base pressure is often the simplest and most effective method of reducing drag. Consequently, base bleed technology becomes a great solution for increasing the range of medium and high caliber ammunition.

2.1.1 Base Bleed

Developed in the mid-1960s in Sweden, the base bleed technology principle is the injection of gases into the base of the projectile, through the combustion of a propellant grain, which increases the pressure and reduces the base drag. For example, as seen in the flow field shown in Fig. 2(a), a region of low pressure is created behind the projectile and causes shock waves due to changes in the flow direction. Thus, a large recirculation zone appears behind the base and causes the drag (Anderson *et al.*, 1976; Serdarevic-Kadic and Terzic, 2019).

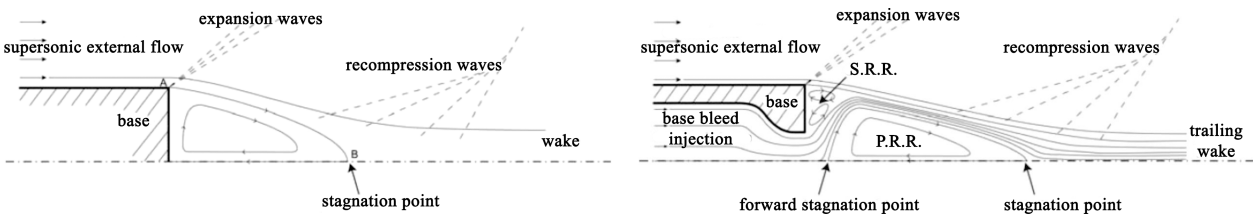

(a) without base bleed; (b) with base bleed.

Figure 2. Flow field behind a projectile (Serdarevic-Kadic and Terzic, 2019)

Now, as illustrated in Fig. 2(b), it can be observed that the addition of a base bleed unit to the projectile divides the recirculation zone into two smaller zones. The injection of gases into the flow field increases the pressure at the base and the smaller pressure difference decreases the recirculation zones and the effects of flow direction changes, consequently decreasing the base drag (Serdarevic-Kadic and Terzic, 2019).

However, gas injection in the flow field can increase or decrease the base pressure. Thus, the base bleed injection cannot exceed the value for which the pressure increase is maximum, as shown in Fig. 3 (Anderson *et al.*, 1976).

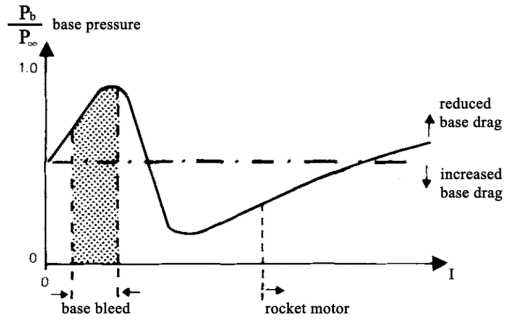

Figure 3. Base pressure dependence of gas injection (Anderson *et al.*, 1976)

The range increase using a BB system can exceed 25%, according to tests performed by Anderson *et al.* (1976). Therefore, it is possible to understand the importance of the base bleed technology since, in addition to being a simple and inexpensive solution, it presents excellent results in range extension.

Furthermore, it is interesting to highlight the studies carried out by Mahmoud *et al.* (2013), whose results show that it is possible to improve the range increase of the BB system. Called live base bleed, the system works by using a propellant with different burning rates.

Figure 4 shows a comparison between the trajectories obtained for the live BB, in simulations and experimental tests, and for the original BB munitions that evidences the effectiveness of the live system. The greatest range increase is obtained through a greater propellant mass flow rate at the base of the projectile in the initial instants combined with a slower burn in the latter stage to endure gas injection for the most part of the upward movement (Mahmoud *et al.*, 2013).

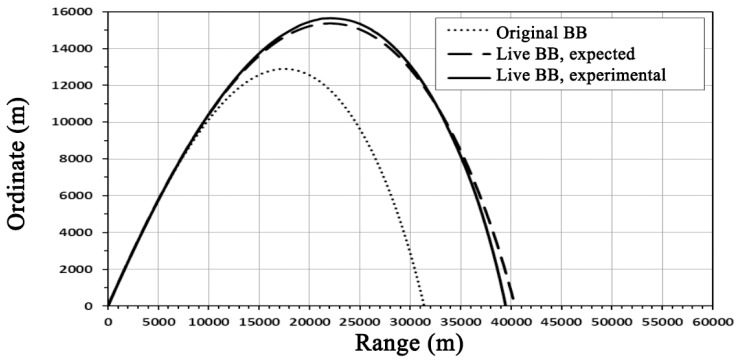

Figure 4. Comparison between trajectories for original and live base bleed (Mahmoud *et al.*, 2013)

3. BALLISTIC TRAJECTORY

The study of the trajectory can be carried out using various trajectory models, which are differentiated by the different aerodynamic forces and moments considered. The simplest model, the point-mass, does not explain phenomena such as drift and induced lift force. On the other hand, the rigid body model, despite producing quite consistent results with the physical experiments, requires a lot of time and computational resources (McCoy, 2012).

For this reason, it was developed the modified point-mass trajectory model (MPMTM), which is significantly less onerous than the rigid-body model and produces satisfactory results. The model replaces the 3 degrees of freedom (DOF) for rotations with just one, the rotation of the projectile around its axis of symmetry. Together with the yaw of repose, the 4 DOF allow the reproduction of effects caused by moments in the body during flight (Lieske and Reiter, 1966).

Therefore, in accordance with the STANAG 4355 (2009), the ballistic trajectory analysis will be carried out with the implementation of the MPMTM, which will be presented in this section. The structuring of the equations of motion starts from the definition of the adopted frame of reference, then the formulations of the forces acting on the center of mass are defined and, finally, the distinctive parameters of the adopted model are described, the spin and the yaw of repose.

3.1 Equations of Motion

First, in order to apply standardized equations, it is important to determine a fixed inertial frame of reference against which the position, velocity and acceleration vectors will be defined. According to the NATO agreement, all vectors must have as reference a orthonormal, ground-fixed Cartesian coordinate system defined by unit vectors as shown in Fig. 5.

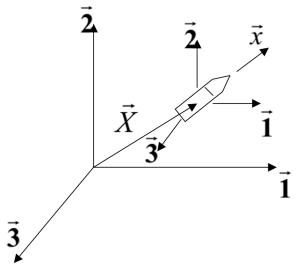

Figure 5. Cartesian Coordinate System with Unit Vectors (NATO, 2009)

In external ballistics studies, the adopted frame of reference has its origin fixed in the muzzle of the weapon. The projectile is also considered a solid of revolution and the unit vector in the axial symmetry direction is defined as $\mathbf{x}$.

Then, having defined the frame of reference, it is also important to define the velocity vectors. The velocity of the projectile with respect to the fixed reference, $\mathbf{u}$, is given by the equation:

$$\mathbf{v} = \mathbf{v_0} + \int_0^t \dot{\mathbf{v}} dt; \qquad \mathbf{v_0} = \begin{bmatrix} \mathrm{v}_0 \cos(QE) \cos(Az) \\ \mathrm{v}_0 \sin(QE) \\ \mathrm{v}_0 \cos(QE) \sin(Az) \end{bmatrix} \tag{1}$$

Where $\mathbf{v}_0$ is the initial velocity vector, a function of the initial flight velocity v_0, the shot elevation angle QE and the launch azimuth Az.

The trajectory model to simulate the flight of projectiles stabilized by rotation is based on the application of Newton's law to analyze the movement of the center of mass which, according to STANAG (2009), suffers the action of forces from base bleed $\mathbf{BB}$, drag $\mathbf{DF}$, lift $\mathbf{LF}$, Magnus $\mathbf{MF}$, coriolis effect $m\mathbf{\Lambda}$ and gravity $m\mathbf{g}$. As the wind speed is disregarded throughout this study for the purpose of simplification, the force equation is:

$$\mathbf{F} = m\dot{\mathbf{v}} = \mathbf{BB} + \mathbf{DF} + \mathbf{LF} + \mathbf{MF} + m\mathbf{\Lambda} + m\mathbf{g} \tag{2}$$

The simulation consists of implementing computational methods to find the position as a function of time from the acceleration vector $\dot{\mathbf{v}}$, given by:

$$\dot{\mathbf{v}} = \frac{\mathbf{BB}}{m} + \frac{\mathbf{DF}}{m} + \frac{\mathbf{LF}}{m} + \frac{\mathbf{MF}}{m} + \mathbf{\Lambda} + \mathbf{g} \tag{3}$$

3.1.1 Gravitational Force

The gravitational force describes the interaction between the body and the Earth's gravitational field. To calculate the acceleration caused by gravity, the model considers the approximation of the spherical Earth and the influence of the latitude on the gravitational force. So the vector $\mathbf{g}$ is:

$$\mathbf{g} = -g_0 \begin{bmatrix} \frac{X}{R_T} \\ 1 - \frac{2Y}{R_T} \\ \frac{Z}{R_T} \end{bmatrix}; \qquad g_0 = 9.80665[1 - 0.0026\cos(2lat)] \tag{4}$$

Where X, Y and Z are the coordinates of the center of mass with respect to the Earth's inertial frame, lat is latitude (negative in the Southern Hemisphere), $R_T = 6.356766 \times 10^6\ m$ is the radius of planet Earth and g_0 represents the variation of gravitational force with latitude.

3.1.2 Coriolis Effect

According to McCoy (2012), the Coriolis effect cannot be disregarded in artillery fire, mainly due to the deflection resulting from this effect, whose acceleration is represented by the vector $\mathbf{\Lambda}$:

$$\mathbf{\Lambda} = -2(\boldsymbol{\omega} \times \mathbf{v}); \qquad \boldsymbol{\omega} = \begin{bmatrix} \Omega \cos(lat) \cos(Az) \\ \Omega \sin(lat) \\ -\Omega \cos(lat) \sin(Az) \end{bmatrix} \tag{5}$$

The vector $\boldsymbol{\omega}$ represents the influence of latitude on the Coriolis effect, with the Earth's angular velocity about the polar axis given by $\Omega = 7.292115 \times 10^{-5}\ rad/s$.

3.1.3 Magnus Force

The Magnus force is a consequence of the asymmetric flow field around the projectile formed by the interaction between the viscous air and the surface of the rotating body. The acceleration of the center of mass due to this force can be calculated by:

$$\frac{\mathbf{MF}}{m} = -\frac{\pi\rho d^3 p}{8m} C_{mag-f} Q_M (\boldsymbol{\alpha}_e \times \mathbf{v}) \tag{6}$$

In the equation above, the parameters are: the projectile mass m; air density ρ; projectile reference diameter d; Magnus force coefficient C_{mag-f}; Magnus force fitting factor Q_m; spin p; and yaw of repose α_e. These last two concepts will shortly be discussed in more detail.

3.1.4 Lift Force

During the flight, the angle between the direction $\mathbf{x}$ and the direction of the projectile's trajectory causes an asymmetric flow around the body and, due to the pressure difference in this flow, there is a lift force, whose acceleration is given by:

$$\frac{\mathbf{LF}}{m} = \frac{\pi\rho d^2 f_L}{8m} (C_{L_\alpha} + C_{L_{\alpha^3}} \alpha_e^2 + C_{L_{\alpha^5}} \alpha_e^4) \mathrm{v}^2 \boldsymbol{\alpha}_e \tag{7}$$

Where f_L is the lift factor and α_e is the magnitude of the yaw of repose. The term C_{L_α} is the lift force coefficient, $C_{L_{\alpha^3}}$ is the cubic lift force coefficient, and $C_{L_{\alpha^5}}$ is the quintic lift force coefficient.

3.1.5 Drag Force

The drag force, which opposes the projectile's trajectory due to the pressure difference in the flow field and the friction between the fluid and the body, is the most important aerodynamic force in studies of range increase.

The acceleration resulting from the drag force can also be given as a function of the form factor or the ballistic coefficient, but in the present study it will be calculated as a function of the drag factor, according to the equation:

$$\frac{\mathbf{DF}}{m} = -\frac{\pi\rho d^2}{8m} (f_D C_{D_0} + C_{D_{\alpha^2}} (Q_D \alpha_e)^2 + C_{D_{\alpha^4}} (Q_D \alpha_e)^4) \mathrm{v}\mathbf{v} \tag{8}$$

Given the parameters: drag factor f_D; zero-yaw drag force coefficient C_{D_0}; quadratic drag force coefficient $C_{D_{\alpha^2}}$; quartic drag force coefficient $C_{D_{\alpha^4}}$; and yaw drag fitting factor Q_D.

3.1.6 Base Bleed

The base bleed system, despite not having the objective of generating thrust, induces acceleration over the center of mass, as shown in Eq. (3). This acceleration, according to STANAG (2009), is calculated by the equation:

$$\frac{\mathbf{BB}}{m} = \frac{\pi\rho d^2 f(i_{BB}, MT)}{8m} C_{x_{BB}} f(I) \mathrm{v}^2 \left(\frac{\mathbf{v}\cos(\alpha_e)}{\mathrm{v}} + \boldsymbol{\alpha}_e \right) \tag{9}$$

Equation (9) has parameters such as the BB factor $f(i_{BB}, MT)$, the BB drag reduction coefficient $C_{x_{BB}}$ and the injection function $f(I)$. Note that the BB factor is a function of yaw drag reduction fitting factor i_{BB} and temperature of motor fuel MT.

Besides, let I_0 be the optimal injection parameter and the parameter I be a function of the mass flow $\dot{m}_f$ and the boat tail diameter d_b, the function of the injection parameter is given by:

$$f(I) = \begin{cases} \frac{I}{I_0}, & I < I_0 \\ 1, & I \geq I_0 \end{cases}; \qquad I = \frac{4\dot{m}_f}{\pi\rho \mathrm{v} {d_b}^2} \tag{10}$$

The BB burning causes a mass flow and, for this reason, other characteristics of the projectile vary, such as the moment of inertia I_x and the location of the center of mass X_{CG}, according to the equations:

$$I_x = I_{x_0} + \left[\frac{(I_{x_0} - I_{x_B})(m - m_0)}{m_0 - m_B} \right] \tag{11}$$

$$X_{CG} = X_{CG_0} + \left[\frac{(X_{CG_0} - X_{CG_B})(m - m_0)}{m_0 - m_B} \right] \tag{12}$$

Where the parameters are: the initial moment of inertia I_{x_0}; the initial location of the center of mass X_{CG_0}; the initial mass m_0; the moment of inertia at BB burnout I_{x_B}; the location of the center of mass at burnout X_{CG_B}; and the mass at burnout m_B.

3.1.7 Spin

The base bleed technology is intended to increase the range of spin-stabilized projectiles by reducing base drag. Thus, the axial rotation of the projectile p, called spin, constitutes an essential part of this study and is calculated by the equation:

$$p = p_0 + \int_0^t \dot{p} dt; \qquad \dot{p} = \frac{\pi \rho d^4 p \mathrm{v} C_{spin}}{8 I_x} \quad and \quad p_0 = \frac{2\pi \mathrm{v}_0}{t_c d} \tag{13}$$

Where $\dot{p}$ is the acceleration of spin, C_{spin} is the spin damping moment coefficient and p_0 is the initial spin of the projectile, a function of the twist rate in the tube t_c.

3.1.8 Yaw of Repose

As seen earlier in this section, the modified point-mass model uses a parameter called yaw of repose to reduce the number of DOF needed to simulate the projectile's trajectory without disregarding the influence of spin and drift.

With the linear and cubic overturning coefficients, C_{M_α} and $C_{M_{\alpha^3}}$ respectively, the vector $\boldsymbol{\alpha}_e$ is calculate by:

$$\boldsymbol{\alpha}_e = -\frac{8 I_x p}{\pi \rho d^3} \frac{\mathbf{v} \times \dot{\mathbf{v}}}{(C_{M_\alpha} + C_{M_{\alpha^3}} \alpha_e^2) \mathrm{v}^4} \tag{14}$$

The MPMTM is an implicit method, and for this reason, the initial value of the acceleration $\dot{\mathbf{v}}$ must be estimated to start the numerical solution. This estimate is made assuming a null initial yaw of repose $\boldsymbol{\alpha}_{e_0}$, as:

$$\boldsymbol{\alpha}_{e_0} = \begin{bmatrix} 0 \\ 0 \\ 0 \end{bmatrix} \tag{15}$$

4. NUMERICAL SOLUTION

Once the adopted trajectory model is defined, in order to simulate the projectile's flight, it is necessary to define the parameters used and how the numerical solution of the differential equations will be performed. In addition, in this section there is the logic behind the code developed for the simulations.

4.1 Parameters

The projectile's trajectory can be influenced by several parameters such as atmospheric conditions, geometry of the projectile and initial shooting conditions. Thus, the definition of parameters is essential to this study.

4.1.1 Atmospheric Conditions

Aerodynamic forces are fundamental to the trajectory model adopted. The air density around the projectile, for example, can be reduced by more than 50% during the flight. Thus, as atmospheric conditions have a great influence on the trajectory, a standard atmosphere manual developed by the International Civil Aviation Organization (ICAO) (1993) was used for the simulation, that considers the atmospheric air as an ideal gas and uses the data found in Tab. 1.

Table 1. Constants and standard values regarding atmospheric conditions ICAO (1993)

Sea level atmospheric pressure	P_0	101.325×10^3 Pa	Specific gas constant (Air)	R	287.05 J · Kg $^{-1}$ · K $^{-1}$
Sea level temperature	T_0	288.15 K	Temperature gradient	β	-6.5×10^{-3} K · m $^{-1}$
Sea level atmospheric density	ρ_0	1.225 Kg · m $^{-3}$	Pressure at 11000m altitude	P_b	22.632×10^3 Pa
Adiabatic index (Air)	K	1.4			

According to the manual (ICAO, 1993), the atmosphere is divided into several layers, at different altitudes. As the object of study is the trajectory of a howitzer shot, it is sufficient to analyze only the first two layers. Thus, it is possible to find the values of temperature and pressure as functions of the height, H, with the following equations:

$$T = \begin{cases} T_0 + \beta \cdot H \\ 216.65 \end{cases} \quad and \quad P = \begin{cases} P_0 \left[1 + \frac{\beta}{T_0} \cdot H\right]^{-\frac{g_0}{\beta R}} & for \;\; H < 11000m \\ P_b \cdot exp\left[-\frac{g_0}{RT}(H - 11000)\right] & for \;\; 11000 \leq H \leq 20000m \end{cases} \tag{16}$$

Once the temperature and pressure are determined, it is possible to find the air density, an essential parameter to calculate aerodynamic forces during flight, by the equation:

$$\rho = \frac{P}{RT} \tag{17}$$

4.1.2 Ballistic Conditions

Ballistic conditions refer to dynamic and geometry characteristics of the projectile that influence flight dynamics, and can be divided into two groups: projectile characteristics and shooting conditions.

The projectile studied was developed by EMGEPRON with the support of PRODAS® and the parameters related to projectile's characteristics needed to perform flight simulations, according to the STANAG (2009), are listed in Tab. 2, that also shows the parameters referring to the initial shooting conditions used. It is important to note that the frame of reference's origin is fixed in the gun muzzle (NATO, 2009) and, for this study, the latitude is from Rio de Janeiro.

Table 2. Projectile characteristics and shooting conditions (Rosendo, 2020)

Reference diameter	d	0.112738 m	Muzzle velocity	v_0	878 m·s^{-1}
Boat tail diameter	d_b	0.10690 m	Angles of elevation	QE	711.1 and 800 mil
Projectile mass (without propellant)	m	19.8190 Kg	Azimuth	Az	0 mil
Propellant mass	m_p	0.5853 Kg	Latitude	lat	$-23\pi/180$ rad
Initial moment of inertia	I_{x_0}	0.03759 Kg·m^2	Rifling twist at muzzle	t_c	25 calibers per revolution
Moment of Inertia after burnout	I_{x_B}	0.03710 Kg·m^2	Yaw drag fitting factor	Q_D	1.2
Initial center of mass	X_{CG_0}	0.407632 m	Magnus force fitting factor	Q_M	1.2
Center of mass at burnout	X_{CG_B}	0.40277 m			

4.1.3 Aerodynamic Conditions

According to Rosendo (2020), the aerodynamic coefficients were calculated using semi-empirical formulations from geometric and mass projectile properties, supported by PRODAS®. Dimensionless variables, these coefficients are functions of Mach number and yaw of repose according Tab. 3. It is important to note that the simulations were performed considering that the lift force and the yaw of repose vary linearly and that the effect of the fourth component of the yaw from rest is negligible, thus the coefficients $C_{L_{\alpha^3}}$, $C_{L_{\alpha^5}}$ and $C_{D_{\alpha^4}}$ are null.

Table 3. Coeficientes aerodinâmicos do *PRODAS*® Rosendo (2020)

Mach	$\mathbf{C_{D_0}}$	$\mathbf{C_{D_{\alpha^2}}}$	$\mathbf{C_{L_\alpha}}$	$\mathbf{C_{M_\alpha}}$	$\mathbf{C_{mag-f}}$	$\mathbf{C_{spin}}$	$\mathbf{C_{x_{BB}}}$
0.01	0.1707	3.98765	1.7923	4.265	-0.415	-0.01294	0.1221
0.4	0.1696	4.0052	1.8104	4.266	-0.415	-0.013075	0.1236
0.7	0.1712	4.1904	1.7848	4.313	-0.42	-0.01298	0.1354
0.9	0.2019	4.91605	1.7951	4.599	-0.46	-0.012685	0.1440
1	0.328	5.868	1.824	4.66	-0.485	-0.01242	0.1849
1.1	0.3712	6.9194	1.9438	4.623	-0.415	-0.012135	0.1822
1.2	0.362	7.495	2.054	4.636	-0.375	-0.01187	0.1791
1.5	0.3251	6.63445	2.2519	4.593	-0.325	-0.01112	0.1678
2	0.2782	5.7819	2.5128	4.39	-0.295	-0.010295	0.1438
3	0.2125	4.76375	2.6075	4.077	-0.29	-0.009015	0.0963
4	0.1901	4.24695	2.4919	3.987	-0.29	-0.00867	0.0639
5	0.1747	3.82265	2.4453	3.927	-0.29	-0.008505	0.0441
6	0.1638	3.6541	2.4122	3.88	-0.29	-0.008405	0.0318
8	0.1556	3.5502	2.3824	3.822	-0.29	-0.00841	0.0186

4.2 Numerical integration

Finally, it is necessary to perform the numerical solution of the trajectory model and, despite requiring considerably less computational resources than the rigid body model, the modified point-mass model still requires high-order methods for the numerical solution. For this reason, the fourth-order Runge-Kutta method (RK4) will be used.

The method consists of estimating the variation of y in a time interval h, called time step, through the calculation of different variations along this step. From the value of the variable, y_n, at the moment t_n, it is possible to determine the value of y_{n+1} using an incremental function given by the weighted average of the variations determined by the equations above. So, we have the RK4 algorithm, which is also applicable to vector functions:

$$\frac{dy}{dt} = f(t, y) \tag{18}$$

$$k_1 = f(t_n, y_n), \;\; k_2 = f(t_n + \frac{h}{2}, y_n + \frac{h}{2}k_1), \;\; k_3 = f(t_n + \frac{h}{2}, y_n + \frac{h}{2}k_2), \;\; and \; k_4 = f(t_n + h, y_n + hk_3) \tag{19}$$

$$y_{n+1} = y_n + \frac{h}{6}(k_1 + 2k_2 + 2k_3 + k_4) \tag{20}$$

4.3 Simulation

In order to get a reference and then study the influence of the base bleed parameters on range increase, the code developed simulate the flights of a projectile with and without the BB system. The code is simple and its structure is represented by the flowchart in Fig. 6.

First, the simulation parameters, the aerodynamic coefficients generated in PRODAS® and the initial conditions are declared. Then, a function is defined to calculate the differential equations of motion related to the MPMTM, according to the STANAG 4355 (2009), considering the adopted atmosphere model. Furthermore, there are functions for the independent calculation of the yaw of repose and the injection parameter for the projectile with BB. In the end, the Runge-Kutta algorithm is implemented and the flight trajectory is traced.

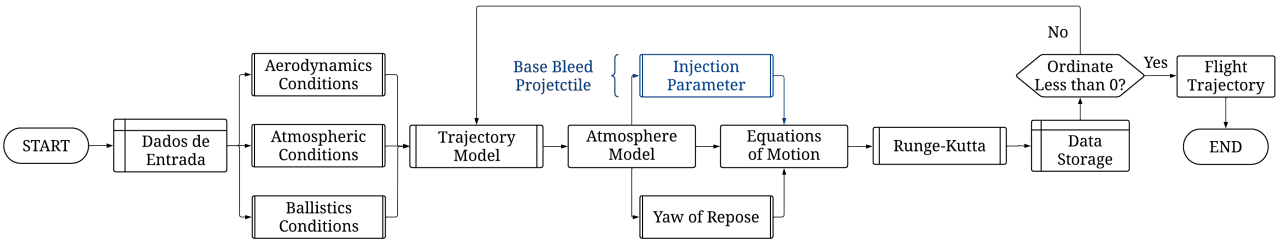

Figure 6. MPMTM simulation code flowchart

5. RESULTS

Initially, the objective was to replicate the trajectory modeling for the projectile without base bleed presented by Rosendo (2020). For this reason, the simulations were performed with the same parameters, which involved considering the coefficients $C_{L_{\alpha^3}}$, $C_{L_{\alpha^5}}$ and $C_{D_{\alpha^4}}$ null and the factors f_L and f_D equal to one.

However, when trying to replicate the trajectories for elevations $711.1\ mil$ and $800\ mil$, the results obtained diverged from the expected. Looking at Fig. 7, it is possible to notice that the difference between the ranges exceeds $1000\ m$ for the increase of $711.1\ mil$ and reaches almost $3000\ m$, for $800\ mil$.

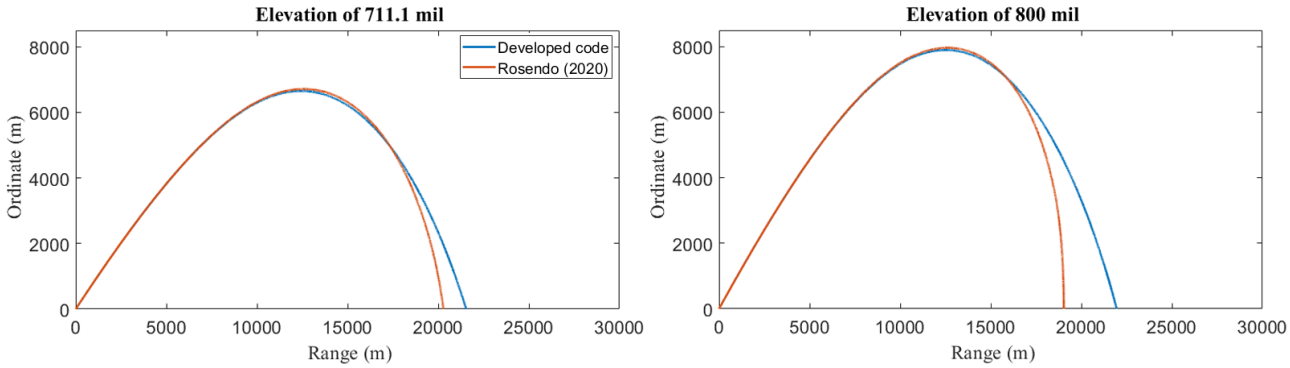

Figure 7. Comparison between the MPMTM trajectories obtained and the ones found by Rosendo (2020)

After some analysis, it was found that the divergence between the obtained and reference results occurred due to an inconsistency in the code used by Rosendo (2020) for his simulations. At an early stage in the development of the simulation code, difficulties were encountered to simulate higher elevation trajectories and, in the search for a solution, an error was identified in the function used for numerical solution, which altered the values of the yaw of repose and caused a deviation from the trajectory.

Therefore, as a way of validating the developed code, simulations were also carried out with the 155 mm M107 howitzer ammunition. In possession of the characteristics of the projectile and the initial ballistic conditions, the range results obtained through the developed code correspond to the values predicted both by PRODAS® and firing tables, as can be seen in Tab. 4, with errors greater than 1% only for high elevation trajectories, where the literature predicts inconsistencies.

Table 4. Results obtained during validation (155 mm M107 ammunition)

PRODAS®				Firing Table			
Elevation	Range (m)		Error	Elevation	Range (m)		Error
(mil)	Expected	Obtained	(%)	(mil)	Expected	Obtained	(%)
58.9	500.0	501.2	0.24	58.9	500.0	501.2	0.24
120.1	1000.0	1001.9	0.19	120.3	1000.0	1003.5	0.35
184.7	1500.0	1501.7	0.11	185.3	1500.0	1506.2	0.41
254.5	2000.0	2001.7	0.09	255.4	2000.0	2007.9	0.40
332.1	2500.0	2501.1	0.04	333.5	2500.0	2509.5	0.38
422.9	3000.0	2999.9	0.00	424.7	3000.0	3008.8	0.29
541.9	3500.0	3498.9	0.03	543.8	3500.0	3505.3	0.15
731.3	3900.0	3897.6	0.06	729.2	3900.0	3896.0	0.11
838.4	3900.0	3898.3	0.05	846.2	3900.0	3891.9	0.21
1027.5	3500.0	3504.3	0.11	1028.3	3500.0	3501.5	0.03
1144.7	3000.0	3016.7	0.53	1141.1	3000.0	3034.3	1.12
1231.4	2500.0	2539.9	1.55	1220.5	2500.0	2605.5	4.18

Finally, after validating the code, the flights of the projectile with base bleed unit were simulated and their trajectories compared with the projectile without BB. Firstly it were analyzed the angles of elevation studied by Rosendo (2020) and the results obtained for range and maximum ordinate increases are listed in Tab. 5 while their trajectories are illustrated in Fig. 8. At this point, it is important to note that the BB factor, $f(i_{BB}, MT)$, and the yaw drag reduction fitting factor, i_{BB}, must be obtained through actual shooting tests in order to adapt them to each simulation performed. However, according to Rosendo (2020), the simulation performed considering the factors equal to one should produce satisfactory results.

Table 5. Range increase with BB

Elevation of 711.1 mil	without BB	with BB	Relative Increase
Range (m)	21547.1	28832.1	33,8%
Maximum Ordinate (m)	6651.8	8620.0	29,6%
Elevation of 800 mil	**without BB**	**with BB**	**Relative Increase**
Range (m)	21957.2	29602.4	34,8%
Maximum Ordinate (m)	7897.8	10383.8	31.5%

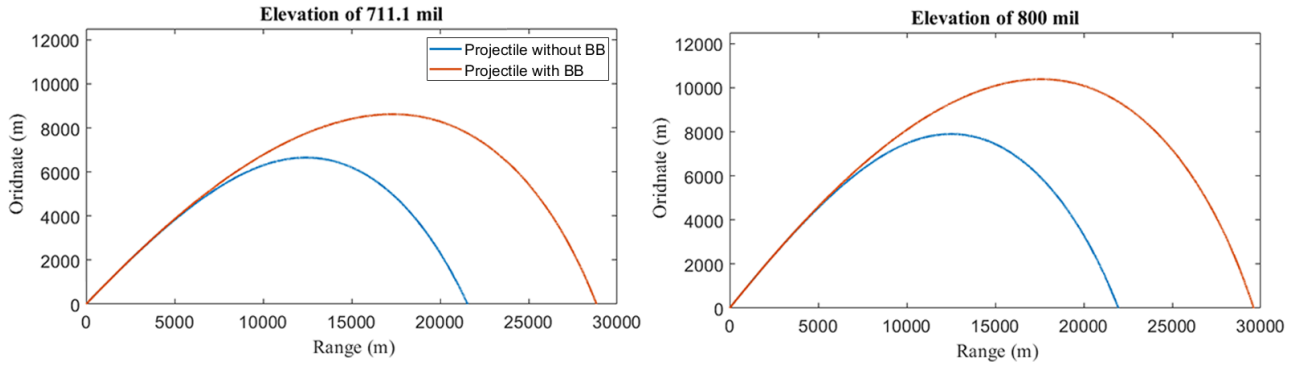

Figure 8. MPMTM trajectories for projectiles with and without BB

Due to the complexity of the BB system, the results were obtained with some simplifications, such as the consideration of a constant mass flow rate of propellant ($\dot{m} = 0.02\,kg/s$) and assigning the value $I_0 = 5 \times 10^{-3}$ to the optimal injection parameter. According to Rosendo (2020), who used these same parameters in his simulations, they were obtained through static tests simulated in a thermochemistry software.

However, when performing an analysis of the results obtained, it can be noted that the values obtained for range increase are above what is expected in the literature. For example, while the predicted increase is around $25\,\%$, when running the simulation for various elevations, the relative increase reaches $49.7\,\%$ as can be seen in the Tab. 6. Such divergence may occur due to the parameters used for the base bleed system, since they were not obtained through real tests.

Table 6. Range increases for various angles of elevation

Elevation (mil)	Range (m)		Relative Increase
	without BB	with BB	
440	18205.1	23843.7	31.0 %
530	19614.6	25921.8	32.2 %
620	20737.1	27583.9	33.0 %
710	21539.5	28820.3	33.8 %
800	21957.2	29602.4	34.8 %
890	21893.7	29990.2	37.0 %
980	21267.1	29934.3	40.8 %
1070	19979.4	28884.2	44.6 %
1160	17916.7	26391.6	47.3 %
1250	14838.6	22214.3	49.7 %

In any case, the possibility of achieving greater range increases was also studied. According to Mahmoud *et al.* (2013), the base bleed system is more efficient when the mass flow is relatively higher at the beginning of the burn and then decreases so that the burn time extends for most of the upward movement. For this reason, the simulations were performed again with variable mass flow.

The multigrain propellants studied by Mahmoud *et al.* (2013) were sometimes very complex and, as the objective was only to investigate the possibility of a greater increase, a simplified model was used. Therefore, two values were assigned for the mass flow, both constant, $\dot{m} = 0.03\ kg/s$ until half of the propellant mass was burned and then $\dot{m} = 0,01\ kg/s$ for the remainder of the propellant. The results can be seen in Tab. 7 and Fig. 9.

Table 7. Range increase with live BB

Elevation (mil)	Range (m)			Relative Increase		Additional Increase
	Without BB	Original BB	Live BB	Original BB	Live BB	
440	18205.1	23843.7	24627.7	31.0 %	35.3 %	13.9 %
530	19614.6	25921.8	26800.5	32.2 %	36.6 %	13.7 %
620	20737.1	27583.9	28657.9	33.0 %	38.2 %	15.8 %
710	21539.5	28820.3	30169.0	33.8 %	40.1 %	18.6 %
800	21957.2	29602.4	31223.3	34.8 %	42.2 %	21.3 %
890	21893.7	29990.2	31904.0	37.0 %	45.7 %	23.5 %
980	21267.1	29934.3	31929.9	40.8 %	50.1 %	22.8 %
1070	19979.4	28884.2	30920.2	44.6 %	54.8 %	22.9 %
1160	17916.7	26391.6	28312.4	47.3 %	58.0 %	22.6 %
1250	14838.6	22214.3	23802.8	49.7 %	60.4 %	21.5 %

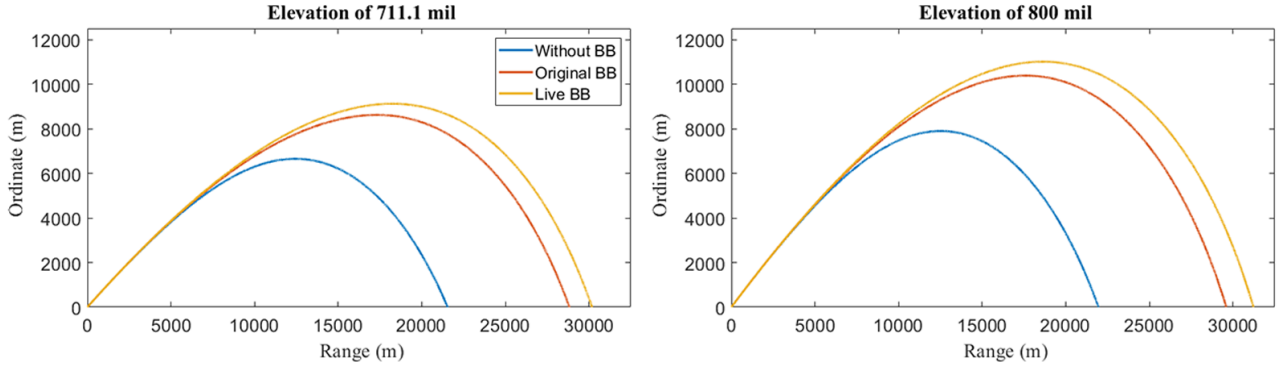

Figure 9. MPMTM trajectories for projectiles without BB, with the original BB and with the live BB

Finally, as can be seen in the table 7, the higher initial mass flow combined with the increase in the total burn time contributed to a higher range increase in all cases. From the analysis of the additional increases, it can be seen that the live base bleed promotes, on average, $20\,\%$ more increase in relation to the BB originally used. However, the values found for the range increases, which now exceed $50\,\%$, are much higher than expected and reinforce the hypothesis of inconsistency in the base bleed system parameters considered initially.

6. CONCLUSIONS

Increasing the range of artillery has become increasingly important, however, despite being used in several countries, Brazil still does not master the technology of extended range ammunition. For this reason, in the course of this project, a study was carried out on increasing the range of ammunition using a base bleed system, through the analysis of trajectories.

Initially, a literature review made it possible to recognize the advantages of the BB technology. It was found that, despite not promoting the greatest range increase possible, the base bleed system is a simple and relatively inexpensive solution that promotes range while maintaining good accuracy and the ability to accommodate explosive charge.

Then, before starting the flight simulations, the ballistic trajectory and some of the parameters that influence the flight dynamics of a projectile were studied. Moment in which greater attention was given to the STANAG 4355, which standardizes ballistic trajectory modeling, and to the MPMTM, model adopted by the standardization agreement due to the good relationship between the accuracy of the results produced and its computational cost.

Finally, the code was developed in MATLAB® for the trajectory simulation of projectiles with and without BB system. The initial objective was to replicate the trajectories obtained by Rosendo (2020), but an inconsistency was found in the code used as a reference. The error was found in the numerical solution that changed the value of the yaw of repose, a essential parameter of the MPMTM, at each iteration and caused a deviation in the trajectory.

Thus, in order to validate the code developed as a means of analyzing the trajectory, simulations were also carried out with the 155 mm M107 howitzer ammunition. And, considering that the range results obtained correspond to the values predicted both by PRODAS® and firing tables, the code is in fact a tool to perform the desired analyses.

As for the results obtained in the simulations with the base bleed system used by Rosendo (2020), the increase values close to $30\,\%$ found for the highlighted elevations are acceptable. However, this increase continues to grow to almost $50\,\%$, values well above the theoretically expected that reveal an inconsistency in the parameters used for the BB.

Furthermore, the study also revealed an opportunity for improvement through the use of live base bleed, a BB system with variable mass flow. From the simulations carried out, it was possible to observe that a higher initial mass flow combined with a longer burn time contribute to an even greater range increase, around $20\,\%$ more than the original BB.

Finally, throughout the project, is was developed a code that allows the study of range increase through trajectory analysis. However, in future studies it is still needed to investigate the parameters of the base bleed system, such as the fitting factors for example, so that the results are more representative of reality, as well as studying the live BB in order to obtain an optimal range increase.

7. REFERENCES

Anderson, K., Gunners, N.E. and Hellgren, R., 1976. "Swedish base bleed - increasing the range of artillery projectiles through base flow". *Propellants and Explosives*, , No. 1, pp. 69–73.

Dali, M.A. and Jaramaz, S., 2018. "Various methods of artilllery projectiles base drag reduction". *8th International Scientific Conference on Defensive Technologies*.

ICAO, 1993. *Manual of the ICAO Standard Atmosphere: extended to 80 kilometres*. Montreal.

Lieske, R.F. and Reiter, M.L., 1966. "Equations of motion for a modified point mass trajectory". Technical Report 1314, Maryland.

Mahmoud, O.K., Abou-Elela, H.A., Ibrahim, A.Z. and Abdel-Hamid, O.E., 2013. "Ballistic analysis of a projectile provided with base bleed unit". *15th International Conference on Aerospace Sciences Aviation Technology*.

McCoy, R.L., 2012. *Modern Exterior Ballistics: The Launch and Flight Dynamics of Symmetric Projectiles*. Schiffer Publishing Ltd., Atglen, 2nd edition.

NATO, 2009. *STANAG 4355: The Modified Point Mass and Five Degrees of Freedom Trajectory Models*. Brussels.

Rosendo, W., 2020. "Numerical solutions for a ballistic trajectory with drag reduction provided by a base bleed unit". *18th Brazilian Congress of Thermal Sciences and Engineering*.

Serdarevic-Kadic, S. and Terzic, J., 2019. "Preliminary design method for base bleed unit". *DAAM International Scientific Book*, , No. 5, pp. 55–70.

8. RESPONSIBILITY NOTICE

The authors are solely responsible for the printed material included in this paper.